European Review for Medical and Pharmacological Sciences 2023; 27: 6510-6522

Auto interpretable depth learning model to analyze the hemodynamic changes and pulmonary complications in laparoscopic gynecologic tumor surgery with nalmefene hydrochloride combined with general anesthesia

L.-T. WANG, A.-R. ZHANG, Q.-Q. WANG, B. BAI

Department of Anesthesiology, Cangzhou People's Hospital, Cangzhou, China

Abstract. – OBJECTIVE: In this work, based on intelligent computing, the biological signals of patients were analyzed to investigate the hemodynamic changes and pulmonary complications of Nalmefene Hcl combined with general anesthesia (GA) in laparoscopic gynecological tumor surgery (GTS).

PATIENTS AND METHODS: Eighty computer-aided GTS patients were randomly divided into a control group (n = 40) and an observation group (n = 40). Biomedical electrocardiogram (ECG) signals were detected by wavelet neural network in all patients undergoing laparoscopic gynecological tumor surgery and were computerized according to the android interface definition language model (AIDL). GA was used during surgery. The observation group was injected intravenously with 0.2 μg/kg naproxenacin hydrochloride after operation. The control group was given 1 mL 0.9% sodium chloride solution after operation. Mean arterial pressure (MAP), heart rate (HR), respiratory rate (RR), pulse oxygen saturation (SPO), coma score, and adverse reactions (AR) were compared between the two groups at 10, 20, and 30 minutes after wakefulness. The hemodynamic parameters between the two groups were compared. Serum urocholine (URO) and creatinine (Cre) levels were analyzed in patients without complications.

RESULTS: ECG waveform based on wavelet neural network has a high recognition rate and strong generalization ability. 37 patients in the observation group recovered within 10 minutes after surgery, and the recovery rate at 30 minutes was 95%. 30 patients in the control group awoke 10 minutes after the operation, and the recovery rate at 30 minutes m-AR was 75%. The average abstract windows toolkit (AWT) of the observation group and control group was 11.87 ± 5.78 min and 16.46 ± 5.32 min, respectively, and the difference was significant ($p < 0.05$). There were significant differences in HR, systolic blood pressure (SBP), and diastolic blood pressure (DBP) between the observation group and the control group during the extubation ($p < 0.05$). Blood gas indexes PaO_2, PvO_2, $PaCO_2$, and $PvCO_2$ in the observation group were significantly different from those in the control group half an hour after the operation and half an hour after pneumoperitoneum ($p > 0.05$).

CONCLUSIONS: Intelligent computational biological signal detection was beneficial to the development of surgery. Nalmefene Hcl combined with GA on the basis of the AIDL model has a significant effect on the awakening of GTS patients and can shorten sleep time. Patients with underlying cardiac disease were more likely to develop postoperative lung complications.

Key Words:

Auto interpretable depth learning model, General anesthesia, Gynecologic tumor, Hemodynamic parameters, Pulmonary complications.

Introduction

Laparoscopic surgery is a minimally invasive surgical method. This type of surgery has become widely used to operate on gynecological diseases. Laparoscopy has many advantages, including small trauma, quick postoperative recovery, and small impact on patients, and has been widely used in clinical practice[1,2]. In gynecological laparoscopic surgery, good analgesia and muscle relaxation, as well as physiological changes caused by artificial pneumoperitoneum are required to be alleviated or relieved[3,4]. Rational anesthesia can effectively relieve the pain of patients, effectively reduce the stress response, shorten the operation time, and play a very important response in the expectation of the surgery[5]. Hemodynamic

Corresponding Author: LingTong Wang, MD; e-mail: wanglt067@163.com

changes can cause a series of viscous factors in the blood. The dilatation of the lower extremity veins slows blood flow under the influence of anesthetic drugs[6]. Nalmefene Hcl (17-cyclopropyl methyl 4, 5-epoxy-methylene moran-3, 14-diol) has been used for nearly 20 years, successfully replacing naloxone. It has a long half-life, fast onset, more routes of administration, a wide range of safety, low efficiency, and fewer adverse reactions (ARs). In clinical practice, Nalmefene Hcl is widely used and suitable for waking up after surgery, and the incidence of ARs is less than 1%[7]. As a new generation of opioid receptor antagonists for neuroprotective therapy, Nalmefene Hcl has a longer metabolic time than traditional naloxone and has been applied in septic shock and chronic respiratory failure[8]. Some research[9] results show that Nalmefene Hcl is safe and reliable. The reasons for the delayed awakening of patients after general anesthesia are different, and the treatment methods in clinical practice are also different. Nalmefene Hcl is used to wake up patients, especially for those who have been confirmed to have delayed awakening after surgery, rather than a common way to accelerate GA[10]. With the continuous development of anesthesiology technology, a relatively perfect level has been reached up to now, but further research is needed to explore whether patients can recover quickly after GA[11,12]. Pulmonary complications are also clinically common after an operation, and they may cause serious prognosis. They are the primary complications after abdominal surgery, seriously threatening the life and health of patients[13].

The development of information technology shows the characteristics of digitization, network, and intelligence. The explainability of intelligent computing uses enough comprehensible information to solve a problem, and the explainable depth model can provide a decision-making basis for each prediction result[14,15]. Computational intelligence makes it possible to study the adaptive mechanism of intelligent behavior in complex and changing environments. The methods of computing intelligence include artificial neural network, genetic algorithm, genetic program, evolutionary program, local search, simulated annealing, etc. These algorithms of computational intelligence have the characteristics of self-learning, self-organization, and self-adaptation[16,17]. Biomedical signal processing (BSP) is a new signal-processing method that seeks important information from human physiological signals to guide and diagnose. Intelligent biological signal processing helps us to extract valuable information[18,19]. In medical data processing, interpretability based on intelligent computing can be used to achieve a rapid diagnosis of lesions, greatly shortening the diagnosis time[20]. Wavelet analysis is a very effective technology in signal processing. Neural network and wavelet analysis form a new intelligent information processing method. In the processing of medical, biological signals, the training is simplified to avoid the blindness of network structure design and local optimal nonlinear optimization problems, so as to achieve more obvious results.

Therefore, based on the theory and method of the intelligent algorithm, this work adopted Wavelet Neural Network (WNN) to detect the biomedical ECG signal in patients undergoing laparoscopic gynecological tumor surgery to investigate the hemodynamic changes and pulmonary complications of Nalmefene Hcl combined with GA in automatic vision of gynecological tumor surgery (GTS) and to provide reference for the early recovery of patients during clinical surgery and the improvement of patients' quality of life.

Patients and Methods

Research Objects

80 patients with computer-based GTS admitted to Cangzhou People's Hospital of Hebei Province from 2019 to 2021 were selected and randomly rolled into a control group (n = 40) and an observation group (n = 40). In the observation group, the average age was (41.5 ± 3.61) years old (28 - 50 years old), the average body weight (ABW) was (47.67 ± 4.2) kg (43 - 72 kg), and the average body mass index (BMI) was (23.67 ± 1.2) kg/m^2. There were 3 cases of bilateral tubal formation, 9 cases of ovarian teratoma resection, 10 cases of ovarian cysts, 11 cases of uterine myomectomy, and 7 cases of infertility patients with bilateral tubal fluid. In the control group, the average age was (40.3 ± 3.23) years (27 - 53 years), the ABW was 41.6 - 69 kg, and the average BMI was (23.52 ± 2.4) kg/m^2. No visible difference was observed in general data between the two groups (p > 0.05). The main types of surgery included bilateral tubal formation in 5 cases, ovarian teratoma resection in 11 cases, ovarian cyst in 6 cases, uterine myomectomy in 8 cases, and bilateral tubal fluid in 10 cases of infertility.

The liver and kidney functions of the two groups were normal without obvious anemia and

abnormal blood pressure. The general information, course of disease, and type of disease between the two groups showed no obvious difference. All patients were computerized based on the AIDL model. Intraoperative GA was used. According to the American Society of Anesthesiologists (ASA), all patients were classified as I - II. The patients in the observation group were given Nalmefene Hcl 0.2 μg/kg intravenously to wake up after the operation, while those in the control group were given 1 mL 0.9% sodium chloride solution. The mean arterial pressure (MAP), heart rate (HR), respiratory rate (RR), pulse oxygen saturation (SPO), coma scale, and adverse reactions (Ars) of the two groups were compared at 10 min, 20 min, and 30 min after awakening. The hemodynamic parameters of patients in different groups were compared. The serum urocholine (URO) and creatinine (Cre) levels of patients with and without complications were analyzed.

Objects included in this work had to satisfy the following items: (1) first onset of disease; (2) stable basic vital signs, verbal expression, and clear consciousness; (3) no neuromuscular disease; (4) no abnormalities in blood pressure, heart, lung, liver, and renal function before operation; and (5) gynecologic tumor after computed tomography (CT) or magnetic resonance imaging (MRI) examination. Patients with any of the following conditions had to be excluded: (1) a history of drug dependence and abuse, and alcoholism; (2) previous manic episodes; (3) suffering from mental disorders other than depression; and (4) being unable to receive MRI examination due to their own reasons. All patients who fully met the inclusion criteria accepted the experimental regulations and signed the experimental informed consent, and their families were also informed and agreed to the study. The study was approved by the Ethics Committee of Cangzhou People's Hospital.

Wavelet Neural Network

Wavelet neural network (WNN) is a combination of wavelet analysis theory and neural networks. Wavelet changes can carry out multiscale analysis of signals through scaling and shift transformation and can easily extract local information of signals. The wavelet neural network uses the wavelet element function to replace the neuron and uses the activation function to replace the located wavelet function to replace the Sigmoid function, and establishes the connection between the network coefficient and the wavelet change by an affine transformation. Wavelet change was essentially an integral change between different parameters:

$$M(\vec{s}) = \int_{\Omega} f(\vec{t}) h\left(\vec{s},\vec{t}\right) dt, f(\vec{t}) \in L^2(R) \tag{1}$$

In the above equation (1), $h(\vec{s}, \vec{t})$ represented the wavelet basis, $\vec{t} = (t_1, t_2, ...t_m)$ and $\vec{s} = (s_1, s_2, ...s_n)$ represented the coordinate vectors in the parameter space of m and n dimensions, respectively.

If f(t) was a one-dimensional signal, the wavelet base could be generated according to equation (2):

$$h(x, y, t) = \frac{1}{\sqrt{|x|}} h\left(\frac{t-y}{x}\right) \tag{2}$$

In the above equation (2), x represented the expansion factor, Y was the translation factor, and h(t) referred to the basic wavelet, and $\sqrt{|x|}$ was the normalization coefficient. The size and position of the wavelet base window can be changed by x and y parameters, so as to realize the resolution of the local structure of the signal f(t).

Wavelet neural network is a neural network model constructed based on wavelet analysis. The selected wavelet base was used for linear superposition to achieve signal expression. Signal s(t) was fitted with wavelet base h(x,y,t), and the expression equation was as follows:

$$\vec{s}(t) = \sum_{t=1}^{n} w_n h\left(\frac{t-y_n}{x_n}\right) \tag{3}$$

W_n represented the weight, n represented the number of wavelet bases, x_n referred to the expansion factor of the wavelet base, and y_n stood for the translation factor of the wavelet base.

Network parameters W_n, x_n, and y_n were optimized using the minimum error energy function.

$$Q = \frac{1}{2} \sum_{m=1}^{M} \left(s(t_m) - \vec{s}(t_m)\right)^2 \tag{4}$$

Q was the optimization function value.

The output error Q' equation of the wavelet neural network was expressed as follows:

$$Q' = \frac{\sum_{m=1}^{M}\left(s\left(t_m\right)-\vec{s}\left(t_m\right)\right)^2}{\sum_{m=1}^{M}\left(s\left(t_m\right)\right)^2} \quad (5)$$

The specific implementation steps of the learning algorithm were as follows:

Step 1: Initializing network parameters. The scaling factor, translation factor, network connection weight, learning rate, and momentum factor of the wavelet were assigned initial values. The sample counter P = 1 was entered.

Step 2: Inputting learning sample and corresponding expected output

Step 3: Calculating the output of the hidden layer and output layer

Step 4: Calculating the error and gradient vector

Step 5: Inputting the next sample

Step 6: Identifying whether the algorithm was calculous. If Q was less than a preset precision value, the network learning was stopped; otherwise, it was reset, and the calculation was repeated.

In recognition of ECG signals, the wavelet signal processing ability is to get stronger and stronger, so it can estimate the time and frequency location well. In addition, it can also construct the wavelet neural network model for signal processing along with the nonlinear mapping of neural network, learning ability, and high fault tolerance, which has a good response effect.

Wavelet Neural Network

The Wavelet Neural Network (WNN) is a method that combines wavelet analysis and neural networks. In the context of ECG signal detection, the following steps are involved:

1. Data preparation. ECG signal data is collected and divided into training and testing sets.
2. Feature extraction. Wavelet analysis is employed to extract features from the ECG signals. Wavelet analysis decomposes the signal into sub-signals in different frequency ranges, capturing the signal's time-frequency characteristics.
3. Network construction. The WNN model is constructed using the principles of wavelet analysis and neural networks. By combining these two approaches, the WNN can effectively handle non-linear and time-varying signals.
4. Model training. The WNN is trained using the training set. The training process includes forward propagation and backward propagation, adjusting network parameters to minimize the error between the predicted output and the actual output.
5. Model evaluation. The performance of the trained WNN model is assessed using the testing set. Various metrics such as accuracy, recall, and precision can be employed to evaluate the model's performance.
6. Prediction and detection. The trained WNN model is utilized to predict and detect new ECG signals. The signal is inputted into the network, and the prediction results are obtained through forward propagation.

Research Methods and Main Reagents

Main reagents

Atropine injection (Harbin Pharmaceutical Group Sanjing Pharmaceutical Co., LTD., SFDA approval number: H23021177, China);

Lidocaine (Hebei Yipin Pharmaceutical Co., Ltd., China, SFDA approval number: H20063371, China);

Scopolamine injection (Shanghai Hefeng Pharmaceutical Co., Ltd., SFDA approval number: 96092, China);

Fentanyl (Yichang Renfu Pharmaceutical Co., Ltd., SFDA approval number: 070702, China);

Atracurium (Shanghai Hengrui Pharmaceutical Co., Ltd., SFDA approval number: H20061298, China);

Propofol (Xi'an Libang Pharmaceutical Co., Ltd., SFDA approval number: H19990282, China);

Midazolam (Jiangsu Enhua Pharmaceutical Co., Ltd., SFDA approval number: H19990027, China).

Research methods

Half an hour before surgery, patients were injected with atropine injection 0.5 mg . After the patient entered the operating room, routine tests were performed, including indwelling catheterization, oxygen mask administration, and open venous access. The patients were subjected to epidural anesthesia, and the L1-L2 space of the patients was selected to be pierced vertically, and 2% lidocaine was injected into the catheter at the puncture head 5 mL. The anesthetic drugs can be

selected according to the patient's blood pressure level, and 500 mL lactate Ringer's solution was given to the patient intravenously within half an hour.

For fast HR patients, intramuscular injection of Scopolamine was adopted, and 0.7 mg/kg fentanyl, 0.7 mg/kg atracurium, 2 mg/kg propofol, and 0.04 mg/kg midazolam were used. During the operation, intravenous drugs were given according to the operating conditions. Within 5 minutes, the patient was intubated and connected to the anesthesia machine. During the maintenance of anesthesia, patients were given an additional dose of 5 mL every 45 minutes, depending on the time at which the procedure was initiated.

During the operation, the mask oxygen was given to the patient at a flow rate of 5 L/min, the abdomen was filled with carbon dioxide at 1-2 L/min using an automatic pneumoperitoneum machine, and the abdominal pressure was maintained at 12-14 mmHg. After the operation, the patient was sent to the post-anesthesia testing and treatment room, and Nalmefene Hcl was selected as the wake-up drug for intravenous injection. GA maintenance drugs were stopped before the end of the operation, and routine muscle relaxation and induced breathing were performed after the end of the operation.

Recovery

The observation group underwent lung recruitment before the tracheal tube was removed at the end of the operation, while the control group did not. Specific operations of lung recruitment were as follows. The overflow valve was set at 30 cmH_2O, hand-controlled breathing was ensured, and the balloon was squeezed to maintain an airway pressure of 30 cmH_2O for 20 seconds. After this process was performed fully three times, the mechanical mode could be switched back. After the patient woke up and breathed well, the doctor can unplug the tracheal intubation.

The patient was transported to the anesthesia recovery room, where hypoxemia was recorded. The duration of stay in the anesthesia recovery room, respiratory status, and difficulty in coughing were recorded. Hypoxemia was defined when the patient's SpO_2 on oxygen was lower than 95%, and intervention was required. The incidence of hypoxemia was observed.

A DUSH 4000 monitor (Shenzhen Ningkewode Technology Co., Ltd., Shenzhen, China) was employed to detect HR, and blood gas changes were detected using arterial and mixed venous blood samples. MAP, pulmonary artery pressure (PAP), pulmonary artery wedge pressure (PAWP), cardiac output (CO), cardiac index (CI), and resistance of peripheral vascular (SVR) were detected continuously.

Statistical Analysis

Excel 2007 and SPSS 24.0 (IBM Corp., Armonk, NY, USA) were adopted to input the collected data. The analysis method was selected according to different situations. The measurement data conforming to normal distribution were expressed as mean ± standard deviation (± s), and the inconsistent count data were expressed as frequency and frequency (%). The count data were analyzed by the c^2 test. $p < 0.05$ was considered statistically significant.

Results

ECG Signal Detection Based on Wavelet Neural Network

In the experiment, part of the data provided by the open database was used to verify the classification ability of the wavelet neural network. The ECG signal data obtained from the ECG database are shown in Figure 1.

ECG data were T100 (A), T140 (B) and T220 (C), respectively, and the waveform number was 400. ECG signals identified by wavelet neural network are shown in Figure 2.

Comparison of Hemodynamic Parameters

Before anesthesia, the hemodynamic parameters analysis of the two groups showed that HR, SBP, and DBP of the control group were 83.83 ± 8.67 cycles/min, 129.24 ± 10.18 mmHg, and 71.32 ± 9.87 mmHg, respectively; while those in the observation group were 84.32 ± 8.79 times/min, 128.84 ± 9.08 mmHg, and 72.52 ± 8.89 mmHg,

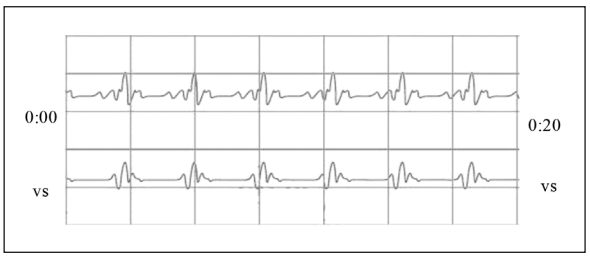

Figure 1. ECG signal waveform.

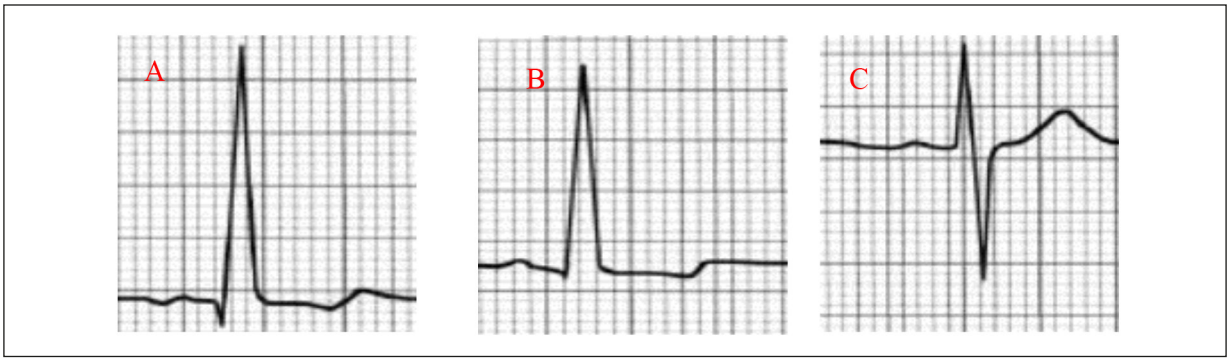

Figure 2. ECG signals of different data. **A**, T100; **B**, T140; **C**, T220.

respectively. Compared with before induction, the results showed $p < 0.05$. The specific results data are given in Figure 3.

During extubation, the HR, SBP, and DBP of the observation group were (84.62 ± 8.97) times/min, (134.64 ± 8.53) mmHg, and (80.36 ± 8.27) mmHg, respectively, while those in the control group were (93.67 ± 8.57) times/min, (148.64 ± 8.93) mmHg, and (92.36 ± 7.76) mmHg, respectively, showing statistically obvious differences ($p < 0.05$). Figure 4 illustrates the above results.

Recovery Parameters in Anesthesia Recovery Room

Among the patients for observation, there was 1 case of hypoxemia (2.5%), 1 case of dyspnea (2.5%), and 3 cases of cough (7.5%) in the anesthesia recovery room. In the observation group, there were 6 cases of hypoxemia (15%), 2 cases of dyspnea (5%), and 4 cases of cough (10%) in the anesthesia recovery room. The difference between the two groups was observable ($p < 0.05$), as demonstrated in Figure 5.

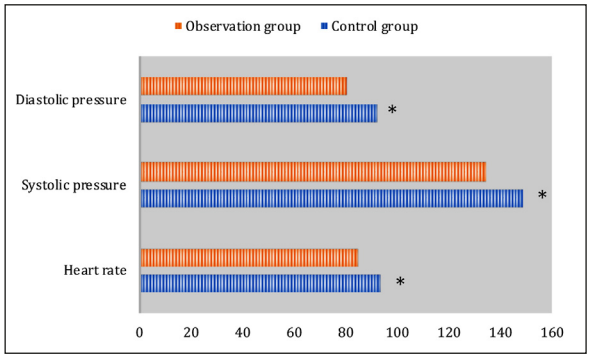

Figure 4. Hemodynamic parameters during extubation (*indicated $p < 0.05$ between two groups).

Awaking Rate

Among the patients in the observation group, 37 cases woke up within 10 minutes after the operation, and 30 m-AR was 95%. Among the patients in the control group, 30 cases woke up for 10 minutes after operation, and the 30 m-AR was 75%. $p < 0.05$ was found in 30 m-AR in two groups, as exhibited in Figure 6.

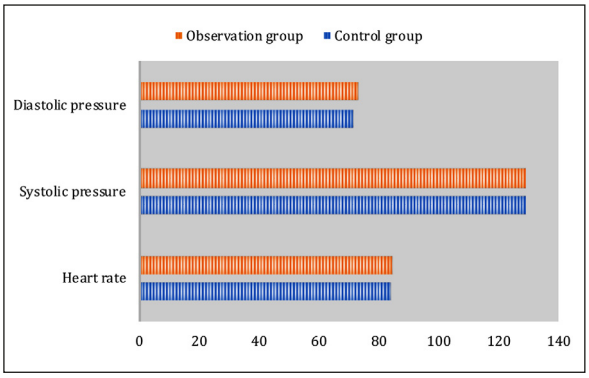

Figure 3. Comparison of hemodynamic parameters before anesthesia induction.

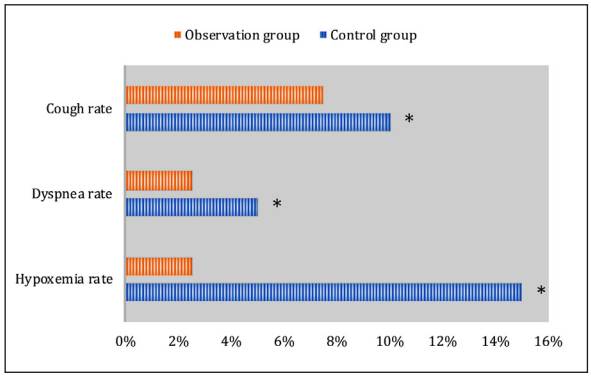

Figure 5. Recovery parameters in the anesthesia recovery room (*indicated $p < 0.05$ between two groups).

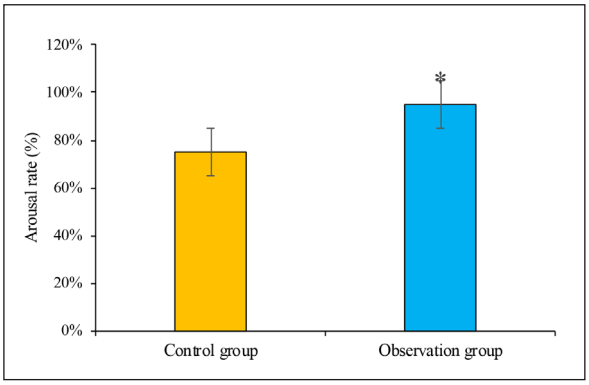

Figure 6. Comparison of awakening rate (*indicated $p <$ 0.05 between two groups).

Figure 7 compares the AWT of patients with different treatment methods. The AWT of the observation and the control group was (11.87 ± 5.78) min and (16.46 ± 5.32) min, respectively, showing $p < 0.05$. The operation time of the observation and the control group was (52.7 ± 8.78) min and (54.8 ± 9.82) min, respectively, showing $p > 0.05$. The pneumoperitoneum time in the observation and control group was (52.7 ± 8.78) min and 54.8 ± 9.82 min, showing $p > 0.05$.

Comparison of Hemodynamic Changes

As illustrated in Figure 8, $p > 0.05$ was found in MAP, PAP, PAWP, CO, and CI between the two groups before anesthesia.

The PAWP, PAP, and MAP of the observation group were higher than those of the control group ($p < 0.05$), and CO and CI exhibited no obvious difference ($p > 0.05$), as exhibited in Figure 9.

As shown in Figure 10, no obvious differences in PAWP, PAP, MAP, CO, and CI were observed between the two groups ($p > 0.05$).

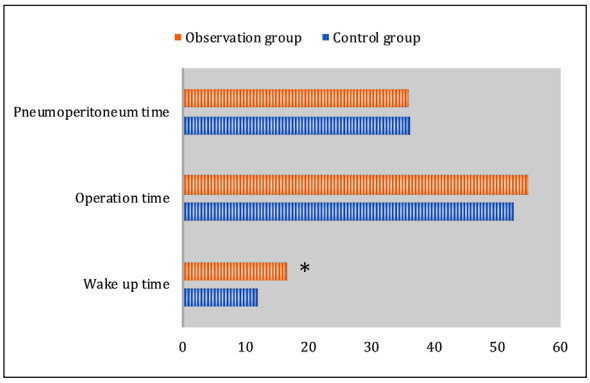

Figure 7. Comparison of wake-up time, operation time, and pneumoperitoneum time (*indicated $p < 0.05$ between two groups).

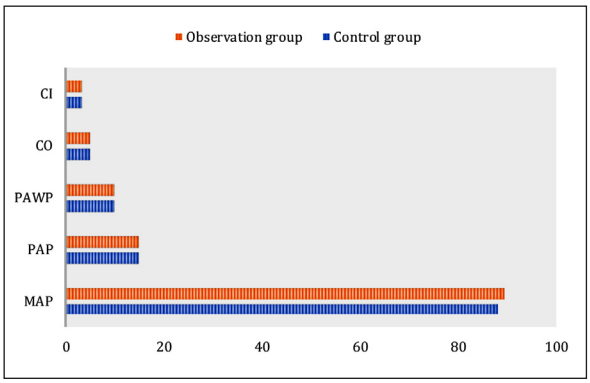

Figure 8. Comparison of hemodynamic changes before anesthesia.

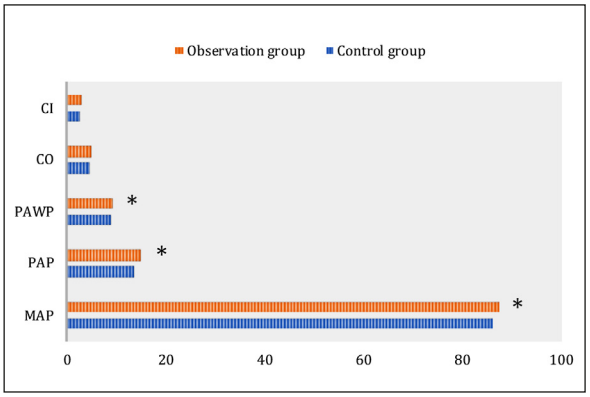

Figure 9. Comparison of hemodynamic changes 20 min after the operation (*indicated $p < 0.05$ between two groups).

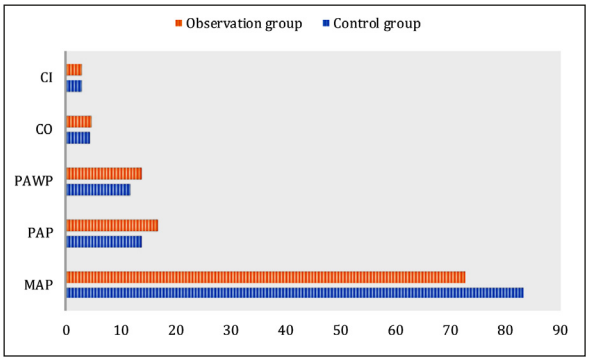

Figure 10. Comparison of hemodynamic changes in 30 min after pneumoperitoneum (*indicated $p < 0.05$ between two groups).

Blood Gas Changes During Anesthesia

Figure 11 suggested that before anesthesia, the PaO_2, PvO_2, $PaCO_2$, and $PvCO_2$ between patients in dif-ferent groups showed $p > 0.05$.

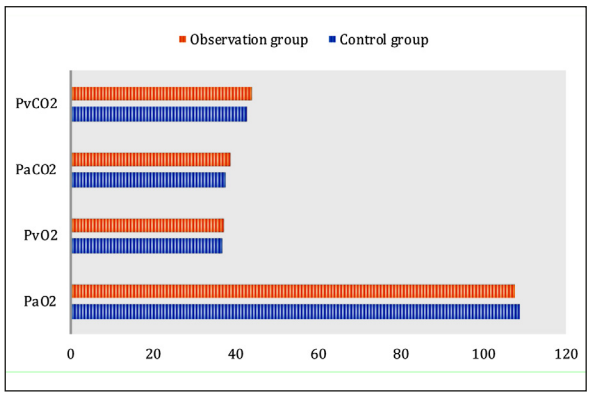

Figure 11. Comparison of blood gas changes before anesthesia.

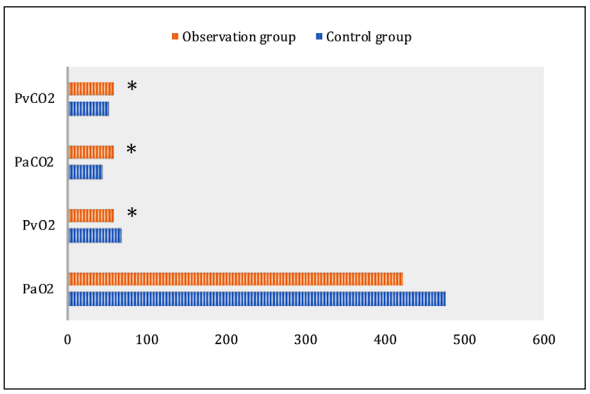

Figure 13. Comparison of blood gas changes 30 min after pneumoperitoneum (*indicated $p < 0.05$ between two groups).

Figure 12 indicated that PaO_2, PvO_2, $PaCO_2$, and $PvCO_2$ in the observation group were significantly different from those in the control group half an hour after operation ($p > 0.05$).

The PvO_2, $PaCO_2$, and $PvCO_2$ of the observation group were sharply different from those of the control group for half an hour after pneumoperitoneum ($p > 0.05$), but the PaO_2 showed $p < 0.05$, as shown in Figure 13.

Case Analysis

Figure 14 shows the CT image of case 1 (female, 63 years old). In Figure 14A, enhanced CT showed a subcapsular liver implant. Figure 14B showed diffuse multilocular cystic implantation along the omentum, peritoneum, and gastrosplenic ligaments, with marked calcification at the gastrosplenic ligaments and a large number of ascites. The red arrow indicates the location of the calcification.

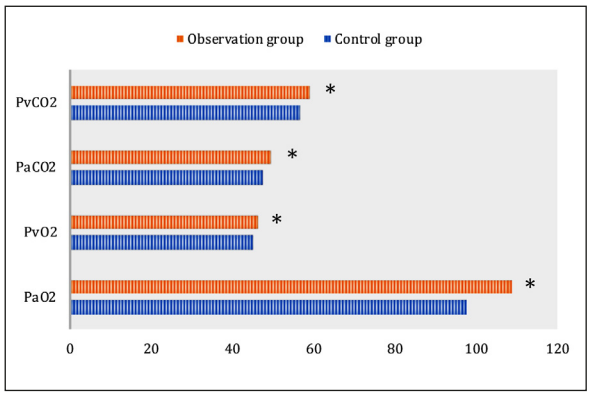

Figure 12. Comparison of blood gas changes 30 min after operation (*indicated $p < 0.05$ between two groups).

Figure 15 shows the image of case 2 (56 years old, papillary serous cystadenoma). Figure 15A showed a multilocular mass near the uterus with irregular substantial components and papillary processes inside the capsule. Figure 15B showed that the signal was enhanced, the papillary process was significantly enhanced, and the degree of enhancement in the parenchymal part was lower than that in the papillary process. The red arrows indicated papillary projections.

Figure 16 shows the images of case 3 (a 41-year-old patient with an ovarian endometrioid tumor). Figure 16A shows a cystic solid mass in the right lower abdomen with partially enhanced parenchyma and irregular wall thickness. Figure 16B showed a thickened endometrial mass with nodular enhancement.

Discussion

The information world has further developed into a holographic world, and intelligent information processing has become a research hotspot in many fields. With the rapid development of science and technology, many systems are becoming more and more complicated, and data accumulation is multiplying. A large amount of data needs to extract superior data information. Intelligent computing systems can collect holographic information from the environment, and intelligent computing can classify the observed data and strengthen the numerical calculation, so as to discover, reason, and identify the result objects predicted by the system[21]. Intelligent computing has been emphasized in the fields of biological signals, computational biology, intelli-

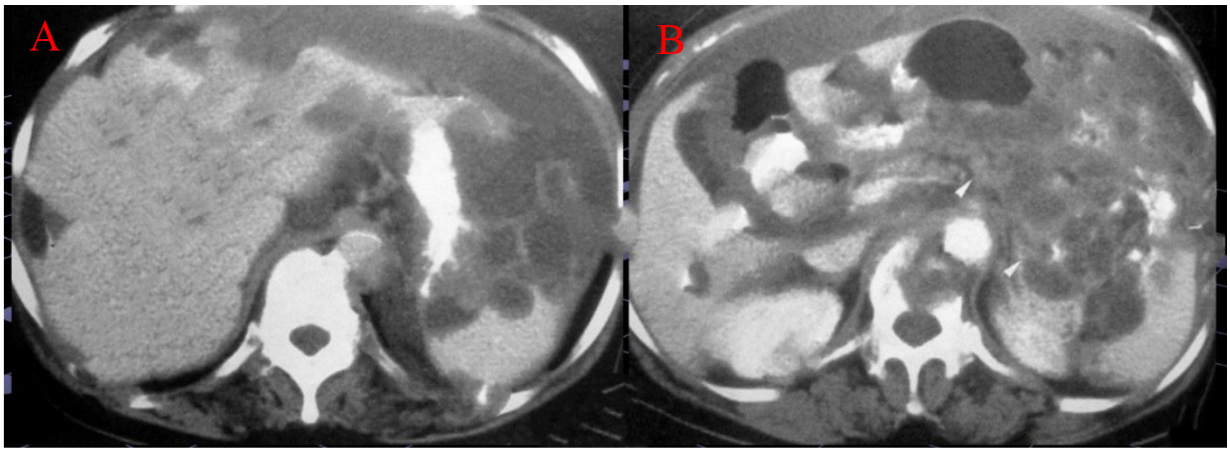

Figure 14. Imaging results of case 1. Red arrow indicates the location of the calcification. **A**, Enhanced CT image of the liver. **B**, Enhanced CT image of stomach and spleen.

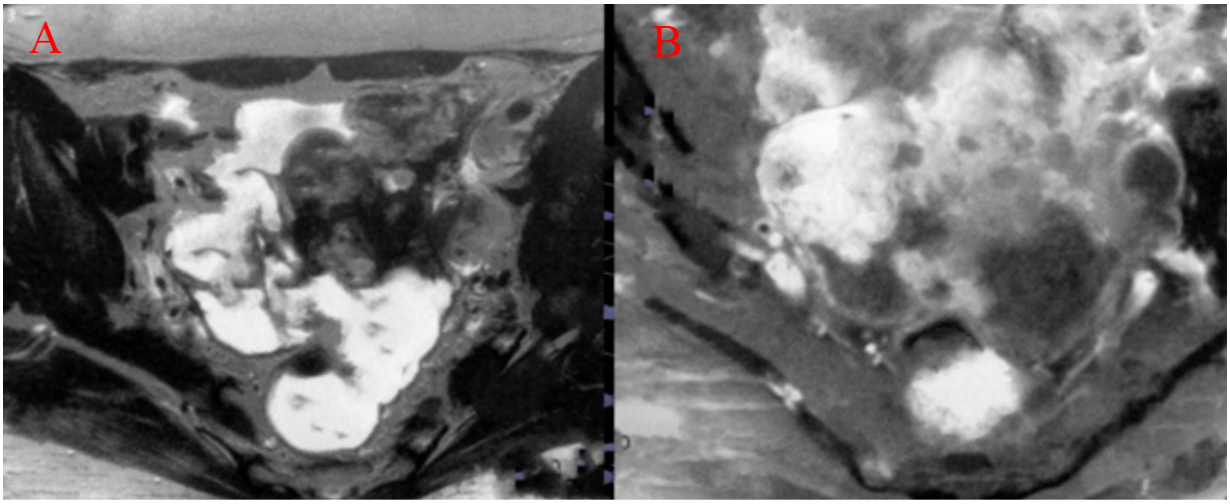

Figure 15. Imaging results of case 2. Red arrows indicate papillary protrusions. **A**, CT image of multilocular mass near uterus. **B**, CT image of papillary serous cystadenoma.

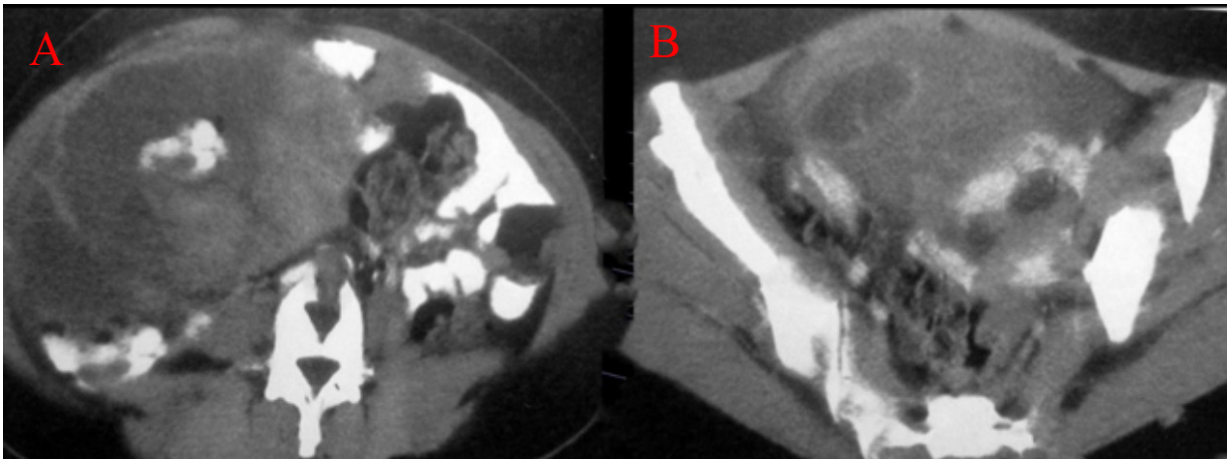

Figure 16. Imaging results of case 3. Red arrow indicates the location of the lump. **A**, Cystic solid mass in the lower right abdomen. **B,** CT image of thickened endometrial mass.

gent game, medical diagnosis, and so on. In this work, wavelet signals and neural networks were combined to detect biomedical ECG signals in patients undergoing laparoscopic gynecological tumor surgery. ECG signals were identified by wavelet neural network using ECG data of T100, T140, T220, and waveform number 400. Wavelet analysis can decompose the signal into sub-signals in different frequency ranges, thus capturing the time-frequency characteristics of the signal. The training set is used to train the wavelet neural network. The training process includes forward propagation and backward propagation, and the error between the predicted output and the actual output is minimized by adjusting the network parameters. The trained wavelet neural network model is used to predict and detect the new ECG signal. The signal is input into the network, and the prediction result is generated through forward propagation. In feature extraction, the time-frequency local features of the wavelet base are given full play, the convergence speed of the wavelet neural network is greatly improved, and the detection ability of non-stationary and nonlinear signals is enhanced. Biometric recognition method is the current research hotspot in the field of pattern recognition. In order to improve the accuracy of ECG signal recognition, many scholars[22] apply intelligent algorithms in biometric intelligent recognition. Li et al[23] found that it can effectively remove noise components and retain the characteristics of ECG signals when denoising ECG data by using scale wavelet transform and an untracked Kalman filter algorithm. Then, the wavelet localization method is used to detect the feature points of the denoised signal, and the obtained feature points are combined with multiple feature vectors to characterize the ECG signal, thus reducing the data dimension in identity recognition. In the whole ECG recognition system, the highest recognition accuracy of a single individual can reach 100%, and the average recognition accuracy can reach 95.17%. Li et al[24] used the wavelet transform algorithm and whale optimization algorithm of probabilistic neural network to identify ECG signals. After intelligent optimization, the accuracy of the model was improved, and the recognition accuracy of a single ECG cycle was 96.97%. Toma et al[25] used a neural network combined with the continuous wavelet transform to convert ECG signals into two-dimensional scale graphs composed of time-frequency components, which improved the arrhythmia detection performance of unbalanced ECG signals and significantly improved the convergence and accuracy of the model. These results indicate that electrocardiogram detection based on an intelligent computing system has good detection performance and can accurately display biomedical signals. Based on the intelligent algorithm, the ECG waveform signals of laparoscopic patients are shown in this work with good results. This also shows the important value of intelligent computing-assisted medical diagnosis.

In this study, the levels of serum urea nitrogen, creatinine, and basic cardiopulmonary diseases in patients with complications were significantly higher than those in patients without complications ($p < 0.05$). During the process of general anesthesia, patients can increase the oxygen flow and adjust the respiratory parameters to reduce $PaCO_2$ and correct the disorder of respiration and circulation. General anesthesia in gynecological laparoscopic surgery can maintain good blood gas status, adjust respiratory and circulatory function, and control the blood pressure of patients. PAP and PAWP returned to normal levels within half an hour after the operation, because the pneumoperitoneum caused the increase in intra-abdominal pressure, which increased the resistance of the peripheral vascular bed and reduced venous blood flow. The change of systemic acid-base balance in patients with normal pulmonary function is rare. Patients with normal cardiopulmonary function can maintain $PaCO_2$ at pre-pneumoperitoneum levels by increasing tidal volume by 25% to 30% of minute ventilation. People with abnormal cardiopulmonary function may increase airway pressure with increasing tidal volume, leading to dramatic hemodynamic changes and barotrauma of the lung. In this work, the complications of postoperative nausea in the control group were higher than those in the observation group, and the patients were in good condition, able to control the respiratory and circulatory function of the patients well and maintain a good blood gas status. The blood gas changes in the observation group were better than those in the control group.

Nalmefene is a morphine receptor-specific blocker with high efficiency, low toxicity, and long action time. It is used in antagonizing respiratory depression, sedation, and hypotension caused by narcotic analgesics. This study showed that Nalmefene Hcl combined with GA could lead to faster recovery time, low influence on patient hemodynamic parameters, and effectively

shorten the operation time. Postoperative pain and other problems are still common phenomena after GA. How to effectively relieve postoperative intravenous analgesia is also a focus of attention. Xiang et al[26] showed that 0.75 mg/kg oxycodone hydrochloride combined with flurbiprofen axetil could provide safe and effective postoperative analgesia for lower abdominal patients with fewer ARs. Wang et al[27] found that oxycodone hydrochloride combined with dexmedetomidine can improve the quality of recovery after anesthesia and reduce stress response in patients undergoing laparoscopic cholecystectomy, which can be safely used in patients undergoing laparoscopic cholecystectomy. Laparoscopic surgery causes less trauma, fast recovery, a short course of the disease, reduces the chance of wound infection, reduces postoperative pain, and restores patients' daily life as soon as possible. Moreover, complications are fewer. Giampaolino et al[28] (2022) analyzed the feasibility of laparoscopic gynecological surgery in regional anesthesia and found it can reduce the influence of surgical pressure and ensure faster recovery without affecting the surgical effect. Although several surgical approaches are available to treat different conditions, local anesthesia technology may be a viable option for carefully selected patients affected by gynecological conditions. The maximum pain score recorded throughout the procedure was 3 out of 5. Local anesthesia has been shown to reduce the effects of surgical stress and ensure a faster recovery without compromising surgical outcomes. Hewitt et al[29] investigated the epidural and local anesthesia sedation, providing a satisfactory condition for laparoscopy-assisted feeding tube placement in healthy dogs. This anesthesia protocol causes less cardiopulmonary depression and may be a better choice for critically ill patients. This work showed that laparoscopic surgery had a good effect on the diagnosis and treatment of gynecologic tumors, which can effectively reduce the hemodynamic indexes of patients and reduce the physical injury of patients. In this work, the blood gas changes between the two groups during anesthesia showed no obvious differences ($p > 0.05$).

Laparoscopy can directly see the real situation of the spread and metastasis of malignant tumors in the pelvis and abdomen, understand the para-aortic and retroperitoneal lymph nodes, and determine the situation of lymph node metastasis. The conditions of laparoscopy for malignant tumors include good laparoscopic operation techniques and a solid basis for diagnosis and treatment of gynecological malignant tumors. The number of lymph nodes removed and positive lymph nodes are comparable to that of an open abdomen, with high safety and fewer complications[30,31]. Sozzi et al[32] (2020) used laparoscopic transverse extended pelvic resection to treat gynecological malignant tumors, and no laparotomy conversion was recorded in the treated patients. R0 resection was achieved in all patients, and the margin was negative. Beuran et al[33] compared the application of laparoscopic and open methods in gynecological abdominal hematoma, and laparoscopic surgery was not inferior to open surgery in the treatment of gynecological acute abdomen. In patients with gynecological benign diseases undergoing laparoscopy, warm water abdominal washing is an important factor in promoting early postoperative anal exhaust[34].

Conclusions

In this study, WNN combined with a neural network model was used to detect biomedical ECG signals in patients undergoing laparoscopic gynecological tumor surgery. ECG waveform based on a wavelet neural network has a high recognition rate and strong generalization ability. Then, the effect of Nalmefene Hcl combined with GA on hemodynamic changes and lung complications in automatic vision GTS was analyzed. Intelligent computational biological signal detection is beneficial to the development of surgery. Nalmefene Hcl combined with GA has a significant clinical effect in the treatment of laparoscopic gynecological tumors. It can reduce the time of lethargy in patients and reduce complications. In addition, patients with underlying medical conditions are more likely to develop lung complications after surgery. The rigorous scientific design of this work, based on the relevant literature, requires further larger prospective trials to evaluate oncology and long-term functional outcomes, which show some theoretical and applied value.

Conflict of Interest

The authors declare that there are no conflicts of interest regarding the publication of this paper.

Ethics Approval

The experimental procedure was approved by the Ethics Committee of Cangzhou People's Hospital, and the ethics approval acceptance number was CZPH0213258.

Informed Consent
The subjects included in this study were all aware of the study and signed informed consent.

Authors' Contribution
All authors of this study participated in the experimental design, sample collection, data statistics, and analysis, and participated in writing, proofreading, text editing, language revision, chart drawing, and final review of the paper.

Data Availability
Data for this work are publicly available in the text, and raw data are available from the authors.

ORCID ID
LingTong Wang: 0009-0003-6183-5351.

Funding
This work is supported by the 2022 Medical Science Research Project Plan of Hebei Provincial Health Commission, Effect of nalmefene hydrochloride on pulmonary function in patients undergoing laparoscopic gynecologic tumor surgery (Project No. 20220325).

References

1) Chiavari R, Pace V, Lambo MS, Volpe D, Fusco P, Marinangeli F. Continuous subarachnoid anesthesia in laparoscopic prostatectomy to enhance hemodynamic stability. Minerva Anestesiol 2022; 88: 416-417.
2) Sakai K, Nakamura M, Yamagami W, Chiyoda T, Kobayashi Y, Nishio H, Hayashi S, Nomura H, Kataoka F, Tominaga E, Banno K, Aoki D. Evaluating the importance of routine drainage following laparoscopic pelvic lymph node dissection for gynecological malignancies. Int J Gynaecol Obstet 2021; 153: 438-442.
3) Wang X, Lin C, Lan L, Liu J. Perioperative intravenous S-ketamine for acute postoperative pain in adults: A systematic review and meta-analysis. J Clin Anesth 2021; 68: 110071.
4) Della Corte L, Mercorio A, Morra I, Riemma G, De Franciscis P, Palumbo M, Viciglione F, Borrelli D, Laganà AS, Vizzielli G, Bifulco G, Giampaolino P. Spinal Anesthesia versus General Anesthesia in Gynecological Laparoscopic Surgery: A Systematic Review and Meta-Analysis. Gynecol Obstet Invest 2022; 87: 1-11.
5) Hajibandeh S, Hajibandeh S, Mobarak S, Bhattacharya P, Mobarak D, Satyadas T. Meta-Analysis of Spinal Anesthesia Versus General Anesthesia During Laparoscopic Total Extraperitoneal Repair of Inguinal Hernia. Surg Laparosc Endosc Percutan Tech 2020; 30: 371-380.
6) Wan Z, Dong Y, Yu Z, Lv H, Lv Z. Semi-Supervised Support Vector Machine for Digital Twins Based Brain Image Fusion. Front Neurosci 2021; 15: 705323.
7) Coll S, Feliu S, Montero C, Pellisé-Tintoré M, Tresserra F, Rodríguez I, Barri-Soldevila PN. Evolution of laparoscopic myomectomy and description of two hemostatic techniques in a large teaching gynecological center. Eur J Obstet Gynecol Reprod Biol 2021; 265: 181-189.
8) Hwang JH, Kim BW. Comparison of General Anesthesia and Combined Spinal and Epidural Anesthesia for Gasless Laparoscopic Surgery in Gynecology. JSLS 2022; 26: e2022.00004.
9) Zhang NL, Wang HQ, Yang J, Yang P, Kang P, Zhao T. Effects of nalmefene hydrochloride on TLR4 signaling pathway in rats with lung ischemia-reperfusion injury. Eur Rev Med Pharmacol Sci 2020; 24: 461-468.
10) Zhou X, Li Y, Liang W. CNN-RNN Based Intelligent Recommendation for Online Medical Pre-Diagnosis Support. IEEE/ACM Trans Comput Biol Bioinform 2021; 18: 912-921.
11) Nagendran M, Chen Y, Lovejoy CA, Gordon AC, Komorowski M, Harvey H, Topol EJ, Ioannidis J, Collins GS, Maruthappu M. Artificial intelligence versus clinicians: systematic review of design, reporting standards, and claims of deep learning studies. BMJ 2020; 368: m689.
12) Le WT, Maleki F, Romero FP, Forghani R, Kadoury S. Overview of Machine Learning: Part 2: Deep Learning for Medical Image Analysis. Neuroimaging Clin N Am 2020; 30: 417-431.
13) Story DA. Computer-assisted Anesthesia Care: Avoiding the Highway to HAL. Anesthesiology 2021; 135: 203-205.
14) Ma S. A Study of Two-Way Short- and Long-Term Memory Network Intelligent Computing IoT Model-Assisted Home Education Attention Mechanism. Comput Intell Neurosci 2021; 2021: 3587884.
15) Zhang X, Shen H, Lv Z. Deployment optimization of multi-stage investment portfolio service and hybrid intelligent algorithm under edge computing. PLoS One 2021; 16: e0252244.
16) Geng H, Yin Z, Zhou C, Guo C. Construction of a simple and intelligent DNA-based computing system for multiplexing logic operations. Acta Biomater 2020; 118: 44-53.
17) Bartolozzi C, Indiveri G, Donati E. Author Correction: Embodied neuromorphic intelligence. Nat Commun 2022; 13: 1415.
18) Paithankar JG, Saini S, Dwivedi S, Sharma A, Chowdhuri DK. Heavy metal associated health hazards: An interplay of oxidative stress and signal transduction. Chemosphere 2021; 262: 128350.
19) Cherupally SK, Yin S, Kadetotad D, Srivastava G, Bae C, Kim SJ, Seo JS. ECG Authentication Hardware Design With Low-Power Signal Processing and Neural Network Optimization With

Low Precision and Structured Compression. IEEE Trans Biomed Circuits Syst 2020; 14: 198-208.

20) An X, Liu Y, Zhao Y, Lu S, Stylios GK, Liu Q. Adaptive Motion Artifact Reduction in Wearable ECG Measurements Using Impedance Pneumography Signal. Sensors (Basel) 2022; 22: 5493.

21) Jiang R, Wu W, Yu Y, Ma F. An Intelligent Control Model of Credit Line Computing in Intelligence Health-Care Systems. Front Public Health 2021; 9: 718594.

22) Yin XX, Hadjiloucas S, Zhang Y, Tian Z. MRI radiogenomics for intelligent diagnosis of breast tumors and accurate prediction of neoadjuvant chemotherapy responses-a review. Comput Methods Programs Biomed 2022; 214: 106510.

23) Li N, Zhu L, Ma W, Wang Y, He F, Zheng A, Zhang X. The Identification of ECG Signals Using WT-UKF and IPSO-SVM. Sensors (Basel) 2022; 22: 1962.

24) Li N, He F, Ma W, Wang R, Jiang L, Zhang X. The Identification of ECG Signals Using Wavelet Transform and WOA-PNN. Sensors (Basel) 2022; 22: 4343.

25) Toma TI, Choi S. A Parallel Cross Convolutional Recurrent Neural Network for Automatic Imbalanced ECG Arrhythmia Detection with Continuous Wavelet Transform. Sensors (Basel) 2022; 22: 7396.

26) Xiang X, Yuan X, Lian Y, Fang J, Wu Y. Effect of oxycodone hydrochloride combined with flurbiprofen axetil for intravenous patient-controlled analgesia in lower abdominal patients: A randomized trial. Medicine (Baltimore) 2018; 97: e9911.

27) Wang GR, Wu Q, Liu WP, Jing YM. Effect of Oxycodone hydrochloride combined with Dexmedetomidine on quality of recovery and stress response after general anesthesia in patients who had Laparoscopic Cholecystectomy. Pak J Med Sci 2021; 37: 1408-1413.

28) Giampaolino P, Della Corte L, Mercorio A, Bruzzese D, Coviello A, Grasso G, Del Piano AC, Bifulco G. Laparoscopic gynecological surgery under minimally invasive anesthesia: a prospective cohort study. Updates Surg 2022; 74: 1755-1762.

29) Hewitt SA, Brisson BA, Sinclair MD, Sears WC. Comparison of cardiopulmonary responses during sedation with epidural and local anesthesia for laparoscopic-assisted jejunostomy feeding tube placement with cardiopulmonary responses during general anesthesia for laparoscopic-assisted or open surgical jejunostomy feeding tube placement in healthy dogs. Am J Vet Res 2007; 68: 358-369.

30) Kendall MC, Castro-Alves LJ. Readmission after lung surgery. J Surg Oncol 2018; 118: 716.

31) Nowak-Psiorz I, Ciećwież SM, Brodowska A, Starczewski A. Treatment of ovarian endometrial cysts in the context of recurrence and fertility. Adv Clin Exp Med 2019; 28: 407-413.

32) Sozzi G, Petrillo M, Gallotta V, Di Donna MC, Ferreri M, Scambia G, Chiantera V. Laparoscopic laterally extended endopelvic resection procedure for gynecological malignancies. Int J Gynecol Cancer 2020; 30: 853-859.

33) Beuran M, Negoi I, Hostiuc S, Catena F, Sartelli M, Negoi RI, Paun S. Laparoscopic Approach has Benefits in Gynecological Emergencies - Even for Massive Hemoperitoneum. Chirurgia (Bucur) 2016; 111: 48-53.

34) Yu M, Wang W, Liu B, Wang N, Gong R, Xu J. Analysis of the operative factors related to anal exhaust time after laparoscopic surgery for benign gynecological diseases. J Gynecol Obstet Hum Reprod 2021; 50: 102142.